Deletion of *kasB* in *Mycobacterium tuberculosis* causes loss of acid-fastness and subclinical latent tuberculosis in immunocompetent mice

Apoorva Bhatt*†‡, Nagatoshi Fujiwara§, Kiranmai Bhatt†¶, Sudagar S. Gurcha‖, Laurent Kremer**, Bing Chen*†, John Chan†, Steven A. Porcelli†, Kazuo Kobayashi§, Gurdyal S. Besra‖, and William R. Jacobs, Jr.*†,††

*Howard Hughes Medical Institute and †Department of Microbiology and Immunology, Albert Einstein College of Medicine, Bronx, NY 10461; §Department of Host Defense, Osaka City University Graduate School of Medicine, Osaka 545-8585, Japan; ‖School of Biosciences, University of Birmingham, Edgbaston, Birmingham B15 2TT, United Kingdom; and **Laboratoire de Dynamique Moléculaire des Interactions Membranaires, Centre National de la Recherche Scientifique, Unité Mixte de Recherche 5539, Université de Montpellier II, 34095 Montpellier Cedex 5, France

Edited by Barry R. Bloom, Harvard School of Public Health, Boston, MA, and approved February 1, 2007 (received for review October 2, 2006)

***Mycobacterium tuberculosis*, the causative agent of tuberculosis, has two distinguishing characteristics: its ability to stain acid-fast and its ability to cause long-term latent infections in humans. Although this distinctive staining characteristic has often been attributed to its lipid-rich cell wall, the specific dye-retaining components were not known. Here we report that targeted deletion of *kasB*, one of two *M. tuberculosis* genes encoding distinct β-ketoacyl- acyl carrier protein synthases involved in mycolic acid synthesis, results in loss of acid-fast staining. Biochemical and structural analyses revealed that the Δ*kasB* mutant strain synthesized mycolates with shorter chain lengths. An additional and unexpected outcome of *kasB* deletion was the loss of ketomycolic acid *trans*-cyclopropanation and a drastic reduction in methoxymycolic acid *trans*-cyclopropanation, activities usually associated with the *trans*-cyclopropane synthase CmaA2. Although deletion of *kasB* also markedly altered the colony morphology and abolished classic serpentine growth (cording), the most profound effect of *kasB* deletion was the ability of the mutant strain to persist in infected immunocompetent mice for up to 600 days without causing disease or mortality. This long-term persistence of Δ*kasB* represents a model for studying latent *M. tuberculosis* infections and suggests that this attenuated strain may represent a valuable vaccine candidate against tuberculosis.**

mycolic acid | Ziehl-Neelsen stain | cording | persistence | FAS-II

The Ziehl–Neelsen stain-based microscopic detection of *Mycobacterium tuberculosis*, which relies on the acid-fast attribute of the tubercle bacillus, remains the cornerstone of diagnosis of tuberculosis (TB), particularly in poor countries where the infection is highly prevalent (1). This staining method was developed by Ziehl and Neelsen who improvised on the early work of Koch, Rindfleisch, and Ehrlich (2–4). Acid-fastness has been attributed to a number of mycobacterial cell wall components, including outer lipids, arabinogalactan-bound mycolic acids (MAs), and free hydroxyl and carboxylate groups of cell wall lipids (5–7). The underlying theme in all of the proposed mechanisms was the presence of a lipid-rich, hydrophobic barrier that could be penetrated by phenol-based stains but was resistant to decolorization by acid-alcohol. However, the precise molecular component responsible for this unique staining property has never been identified.

Early studies on the effects of isoniazid on the staining characteristics of tubercle bacilli demonstrated a loss of acid-fastness after growth in the presence of the antibiotic (8). Because isoniazid was known to inhibit the synthesis of MAs, the major class of lipids composing the cell wall of mycobacteria, this result suggested that these molecules may be the components responsible for the acid-fast staining characteristic and that mutants defective in MA biosynthesis would be reasonable candidates to study the phenomenon of acid-fastness. MAs are very-long-chain α-alkyl β-hydroxy fatty acids that are either esterified to peptidoglycan-linked arabinogalactan or present as a part of the interspersed glycolipid, trehalose dimycolate (TDM) (9, 10). The long mero-MA chain is synthesized by a multienzyme fatty acid synthase II complex (FASII) from acyl carrier protein (ACP)-bound substrates that are elongated by repetitive reductive cycles, the first step of which is catalyzed by a β-ketoacyl-ACP synthase. In *M. tuberculosis* and other mycobacteria, two genes, *kasA* and *kasB*, encode distinct FASII β-ketoacyl-ACP synthases (11). Whereas *kasA* is an essential gene (12), *kasB* is not essential for normal mycobacterial growth in *Mycobacterium marinum* and *Mycobacterium smegmatis* (12, 13), suggesting that *kasB* might be an accessory gene that is not essential for MA biosynthesis. Previous *in vitro* (14) and *in vivo* (13) results had indicated that whereas KasA is involved in the initial elongation of the mero chain, KasB might be responsible for its extension to full-length mero-MAs.

Before this work, the effects of *kasB* deletion in *M. tuberculosis* were unknown, and the role of KasB in pathogenesis had not been investigated in an animal model of infection. In this work, we have shown that the deletion of *kasB* caused alterations in MAs that resulted in a loss of acid-fastness. Furthermore, the *M. tuberculosis* Δ*kasB* mutant was analyzed after infections of both immunocompromised and immunocompetent mice, which revealed a marked attenuation of *in vivo* growth in the mutant that led to a long-term persistent infection that resembled latent tuberculosis. These results provide insights into the nature of the clinically important feature of acid-fast staining in *M. tuberculosis* and are also relevant to understanding and modeling latent tuberculosis.

Results

Deletion of *kasB* Caused a Change in Mycobacterial Colony Morphology and Loss of Cording and Acid-Fastness. A specialized transducing phage, phΔ*kasB*, containing an allelic exchange substrate designed to replace *kasB* with a hygromycin resistance cassette

Author contributions: A.B., J.C., S.A.P., G.S.B., and W.R.J. designed research; A.B., N.F., K.B., S.S.G., L.K., and B.C. performed research; K.K. and W.R.J. contributed new reagents/analytic tools; A.B., N.F., and K.B. analyzed data; and A.B. and W.R.J. wrote the paper.

The authors declare no conflict of interest.

This article is a PNAS direct submission.

Abbreviations: ACP, acyl carrier protein; FASII, fatty acid synthase II complex; MA, mycolic acid; MAME, mycolic acid methyl ester; TB, tuberculosis; TDM, trehalose dimycolate.

‡Present address: School of Biosciences, University of Birmingham, Edgbaston, Birmingham B15 2TT, United Kingdom.

¶Present address: School of Medicine, St. George's University, Grenada, West Indies.

††To whom correspondence should be addressed. E-mail: jacobsw@hhmi.org.

This article contains supporting information online at www.pnas.org/cgi/content/full/0608654104/DC1.

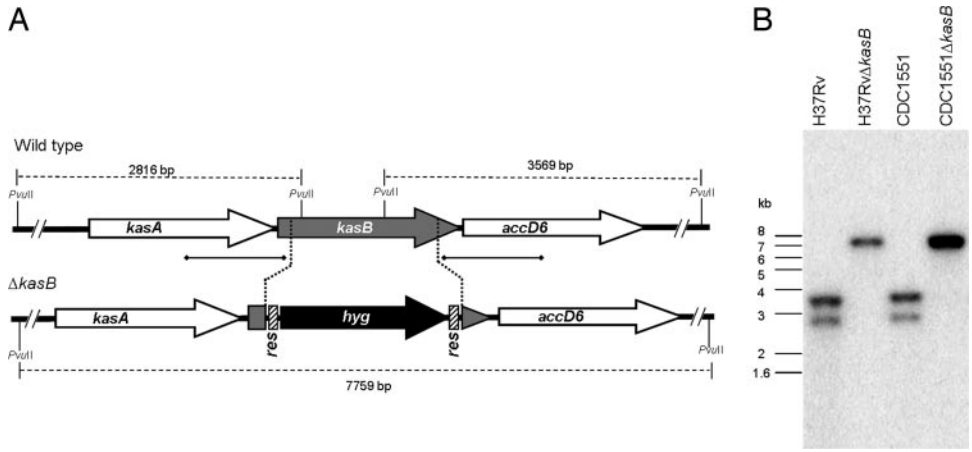

Fig. 1. Generation of a *M. tuberculosis kasB* mutant. (*A*) Map of the *M. tuberculosis kasB* region in WT and Δ*kasB* strains. [α-^{32}P]dCTP-labeled probes were derived from ≈500-bp upstream and downstream flanking sequences that were used to construct the knockout plasmids, and they are indicated by thick lines with square ends. The *PvuII*-digested fragments expected in a Southern blot are indicated by gapped lines with sizes. (*B*) Southern blot of *PvuII*-digested genomic DNA from WT and Δ*kasB* strains. Only one representative band pattern is shown for each mutant strain of H37Rv and CDC1551; *res*, $\gamma\delta$-resolvase site; *hyg*, hygromycin resistance gene.

(*hyg*), was transduced into two virulent *M. tuberculosis* strains, H37Rv (laboratory strain) and CDC1551 (clinical isolate). Southern blot analysis of genomic DNA isolated from hygromycin-resistant (Hyg^R) colonies confirmed replacement of *kasB* with *hyg* (Fig. 1). For further studies, we chose the *kasB* mutant generated in the clinical strain CDC1551; the CDC1551 parental strain, the Δ*kasB* mutant strain, and the complemented strain will be referred to here as WT (wild-type), Δ*kasB*, and Δ*kasB*(pMV261*kasB*), respectively. Deletion of *kasB* resulted in a striking alteration in colony morphology, with the mutant strain forming colonies much smaller than those of the parental strain (Fig. 2). In addition, colonies of mutant strain appeared to have a different surface texture. The smaller size of the colonies was not the result of a slower growth rate because the CDC1551 Δ*kasB* mutant had a doubling rate similar to that of its parental strain when cultured in 7H9 broth (data not shown). WT colony morphology could be restored in the Δ*kasB* mutant upon introduction of *kasB* on a multicopy-replicating plasmid (Fig. 2), indicating that the observed change was due solely to the loss of KasB and not because of a polar effect on the expression of *accD6* located downstream from *kasB*. On the other hand, no complementation was observed with a *kasA*-containing plasmid, indicating that extra copies of *kasA* could not compensate for the loss of *kasB* (data not shown).

A change in colony morphology suggested an altered cell envelope in the Δ*kasB* mutant, and a microscopic examination of cultures grown in 7H9 broth showed that the Δ*kasB* mutant was defective in cording, a classical serpentine growth (Fig. 3). A change in the cell wall composition was further confirmed by acid-fast staining of cultures by two different methods (Kinyoun stain or TB-fluorescent stain), which revealed that the Δ*kasB* strain had lost the ability to retain the primary stain after washing with the acid-alcohol decolorizer (one staining method is shown in Fig. 3). These results suggested that the change in morphology was likely due to a change in the cell wall MA content and correlated well with the increased sensitivity of the Δ*kasB* strain to the lipophilic antibiotic rifampicin (data not shown). The mutant strain was also more sensitive to the KasA/KasB inhibitor thiolactomycin [minimum inhibitory concentration (MIC) <1 μg/ml] than the WT strain (MIC = 5 μg/ml).

MA Chain Length and Cyclopropanation Are Altered in the Δ*kasB* Mutant. The changes in cording and in the acid-fast staining property of the Δ*kasB* strain prompted us to investigate the MA composition of the mutant strain. *M. tuberculosis* produces three classes of MAs: α-, keto-, and methoxy-MAs, each differing in modifications of the mero chain that are catalyzed by distinct cyclopropane synthases, isomerases, and methyl transferases

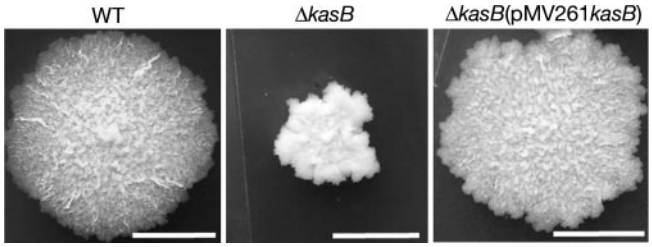

Fig. 2. Colonies of *M. tuberculosis* CDC1551 parental (WT), *kasB* null mutant (Δ*kasB*), and complemented *kasB* mutant [Δ*kasB*(pMV261*kasB*)] strains on 7H10 plates after incubation at 37°C for 4 weeks. (Scale bar, 2 mm.)

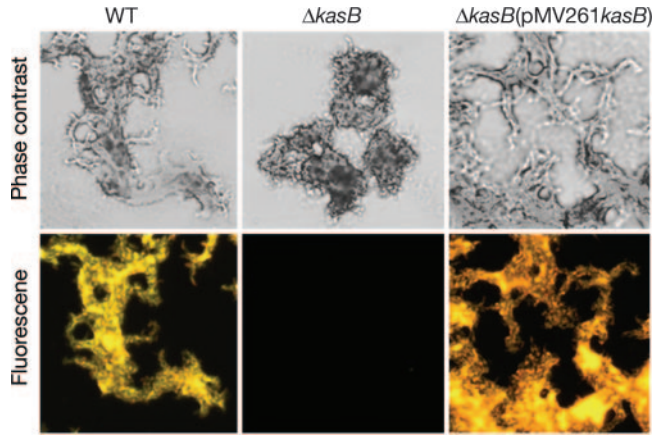

Fig. 3. Light microscopy of *M. tuberculosis* cultures grow static in 7H9 broth at 37°C for 7 days. Cultures were fixed on glass slides, and acid-fast staining was performed on the fixed smears by using the BD TB fluorescent kit-T. (*Upper*) Phase-contrast microscopy images of *M. tuberculosis* WT, Δ*kasB*, and Δ*kasB*(pMV261*kasB*) strains stained with TB-auramine-rhodamine and then treated with acid-alcohol decolorizer. (*Lower*) Fluorescent micrographs of the same fields. (Magnification, ×400.)

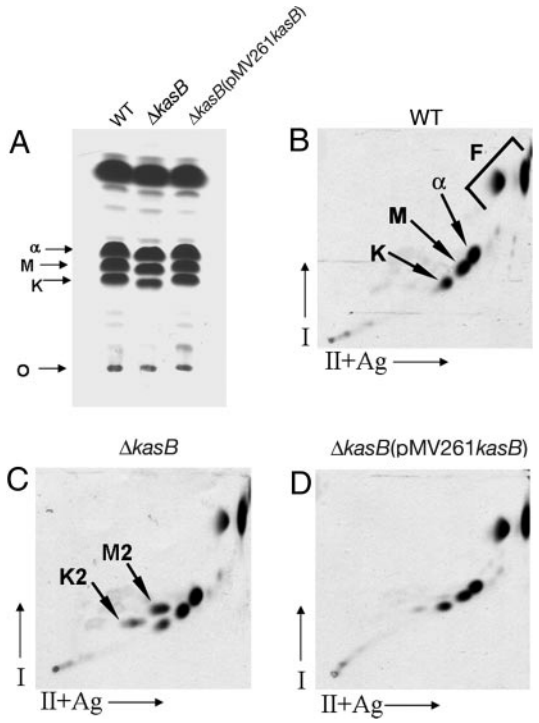

Fig. 4. TLC of ^{14}C-labeled MAMEs from *M. tuberculosis* WT, Δ*kasB*, and Δ*kasB*(pMV261*kasB*) strains. (*A*) Single-dimension HPTLC of MAMEs. (*B–D*) Two-dimensional argentation TLC of WT, Δ*kasB*, and Δ*kasB*(pMV261*kasB*), respectively. O, origin; I, first dimension; II+Ag, second dimension impregnated with $AgNO_3$; α, α-MAMEs; M, methoxy-MAMEs; K, keto-MAMEs; F, fatty acid methyl esters. The two unknown species in the Δ*kasB* strain, M2 and K2, are indicated by arrows.

(15–22). A preliminary analysis of [^{14}C]acetate-labeled MA methyl esters (MAMEs) obtained from total MAs by TLC showed that methoxy- and keto-MAMEs obtained from Δ*kasB* migrated at a slightly lower but reproducible R_f value than those from WT or complemented strains (Fig. 4*A*), suggesting a change in the MA chain lengths. Also, there were differences between the WT and mutant strain with regard to the relative abundance of the three classes of MAMEs: the relative percentages for α-, methoxy-, and keto-MAMEs in total MAMEs from WT strain were 41.5%, 33.5%, and 25%, respectively, and those for the mutant strain were 52%, 32%, and 16%, indicating a decrease in the amount of keto-MAs in the *kasB* mutant [supporting information (SI) Fig. 7]. These defects in MA composition, and the migration in TLCs, were corrected on complementation of Δ*kasB* (Fig. 4*A* and SI Fig. 7). These changes in R_f values and relative abundances of MAs were similar to those observed earlier in a *M. marinum* transposon-disrupted *kasB* mutant (13). Further analysis of MAMEs by two-dimensional argentation TLC (23) (Fig. 4 *B–D*) revealed accumulation of two spots in Δ*kasB* that migrated slightly more slowly than keto- and methoxy-MAME spots in the second dimension (M2 and K2, shown by arrows in Fig. 4*C*). The retarded migration in the second, silver-impregnated, dimension suggested that these spots corresponded to unsaturated MAME species. Similar results were obtained when MAMEs obtained from cell wall-bound MAs and extractable MAs were analyzed separately by two-dimensional TLC, indicating that the altered MAs were esterified to both arabinogalactan and to trehalose (data not shown). No changes in the profiles of other lipids (polar and apolar) were detectable on TLC plates (SI Fig. 8), indicating that the observed phenotypes of Δ*kasB* were likely due to the effects of altered MAs.

Individual MA species were purified from WT, Δ*kasB*, and Δ*kasB*(pMV261*kasB*) and analyzed by MALDI-TOF MS. Spectroscopic data revealed shortened MAs in Δ*kasB* (SI Table 1). The longest α-, methoxy-, and keto-MA species detected in the WT strain were $C_{84:2}$, $C_{92:1}$, and $C_{89:1}$, respectively, whereas in the Δ*kasB* strain the corresponding longest species were $C_{80:2}$, $C_{86:1}$, and $C_{82:1}$, respectively (SI Table 1). In addition, the chain lengths of the most abundant MA species were different in the mutant strain (SI Table 1). Detection of the α-branch by pyrolysis GC revealed that the shortening of chain length was not in the α-branch, but in the mero-MA moiety (SI Fig. 9).

The two accumulated species that were detected by two-dimensional TLC in the Δ*kasB* strain were each found to have a mass identical to the corresponding oxygenated MAME (SI Fig. 10). A more detailed study of purified MAs by ^{1}H NMR analysis revealed the presence of normal levels of *cis*-cyclopropanated methoxy-MAs but diminished resonances for *trans*-cyclopropanated methoxy-MAs in Δ*kasB* (SI Fig. 11). Additionally, no signals corresponding to *trans*-cyclopropanated keto-MAs were detected in the mutant strain (SI Fig. 11).

Furthermore, ^{1}H NMR analysis of total MAs from Δ*kasB* revealed that the two accumulated species in Δ*kasB* were unsaturated precursors of *trans*-cyclopropanated species: signals for *trans*-double bond were detected at 5.24 ppm (*J* 14.7 Hz) and at 5.34 ppm (*J* 14.7 Hz) (24), and the protons for the methylene and the methine groups adjacent to the *trans*-double bond were assigned at 1.96 ppm and 2.01 ppm (15, 25) (SI Fig. 12). The protons of the allylic methyl branch of the proximal *trans*-double bond resonated as a doublet at 0.94 ppm (*J* 6.6 Hz) and the terminal methyl at 0.84 ppm (26, 27). In contrast, spectra of total MAs from the WT strain revealed the absence of allylic methyl branch protons (0.94 ppm) and of *trans*-double bond (5.24 ppm) (data not shown). These results demonstrated that a *trans*-unsaturated precursor of both methoxy- and keto-MAs accumulated in the Δ*kasB* strain.

Loss of KasB in *M. tuberculosis* Causes a Severe Growth *in Vivo* Defect in Mice and Latent Subclinical TB. To assess the effects of altered MAs in the Δ*kasB* strain on mycobacterial virulence, we first tested the ability of the Δ*kasB* mutant to survive in murine (C57BL/6 bone marrow-derived and J774) macrophages and THP-1 cells and found no differences between WT and Δ*kasB* (data not shown). Next, immunocompetent C57BL/6 mice were infected with aerosols of WT, Δ*kasB*, and complemented strains (≈100 bacteria per mouse). Extensive granulomatous inflammation was visible in the lungs of mice infected with the WT or Δ*kasB*(pMV261*kasB*) strains but not in those infected with the Δ*kasB* strain (Fig. 5*A*). Histological examination of stained lung sections from mice infected with the WT or Δ*kasB*(pMV261*kasB*) strains revealed multifocal, moderate infiltration after 21 days of infection (Fig. 5*B*). The severity of the granulomatous lesions increased after 56 days, and after 112 days there was coalescence of lesions into large areas that involved entire lobes of the lung. In contrast, the lungs of mice infected with Δ*kasB* showed more diffuse and less organized infiltrates at 21 days, which decreased in severity after 56 days, and no signs of infection were seen after 112 days (Fig. 5*B*). Consistent with the loss of acid-fastness observed for broth cultures, the *kasB* mutant also failed to retain the primary stain in tissue sections after acid-fast staining and instead took up the methylene blue counterstain (SI Fig. 13).

Monitoring of colony-forming units (cfu) in the lung, spleen, and liver at different time points after infection indicated that the Δ*kasB* mutant was severely attenuated for growth in mice. WT bacteria could replicate extensively in the lung in the first 21 days after aerosol infection, with a three log increase in WT bacteria in infected lungs at the end of 21 days (Fig. 6*A*). In contrast, replication of the Δ*kasB* strain was restricted: bacterial loads in the lung barely increased by 2 orders of magnitude after 21 days of infection and then decreased to between 500 and 1,000

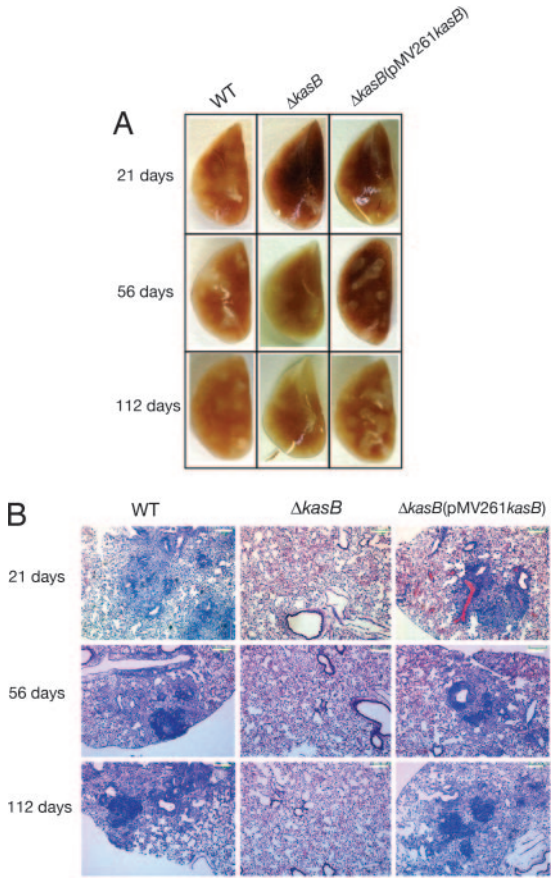

Fig. 5. Pathology of infected mouse lungs. (*A*) Lungs of C57BL/6 mice infected with *M. tuberculosis* WT, Δ*kasB*, and Δ*kasB*(pMV261*kasB*) strains, removed at different time points after aerosol infection. (*B*) Hematoxylin/eosin-stained lung tissue sections from mice infected with WT, Δ*kasB*, or Δ*kasB*(pMV261*kasB*). (Scale bar, 200 μm.)

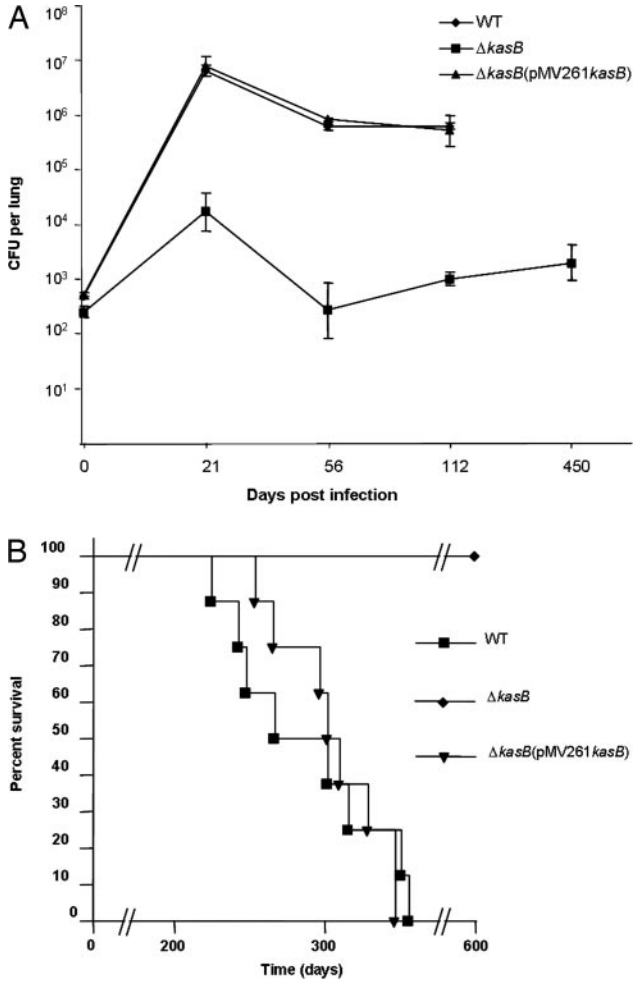

Fig. 6. Attenuation of Δ*kasB* in C57BL/6 mice. (*A*) Plot of *M. tuberculosis* cfu levels in lungs of C57BL/6 mice at different time points after aerosol infection. (*B*) Survival curve of C57BL/6 mice infected with WT, Δ*kasB*, or Δ*kasB* (pMV261*kasB*).

cfu in subsequent weeks (Fig. 6*A*). The Δ*kasB* mutant was also attenuated for growth in liver and spleen (SI Fig. 14 *A* and *B*). Surprisingly, 450 days after aerosol infection, ≈1,000 cfu could still be detected in the lungs of Δ*kasB*-infected mice (Fig. 6*A*), although the mice looked healthy before being killed, which indicated that the mutant was able to persist in the mouse without causing visible signs of disease. Indeed, we observed a significant difference in the mortality of C57BL/6 mice infected by aerosols of the CDC1551 strains (100 cfu per mouse). By day 356, 100% (eight of eight) of the mice infected with WT or Δ*kasB*(pMV261*kasB*) had died (Fig. 6*B*). In stark contrast, all mice infected with Δ*kasB* (eight of eight) were not only alive but also appeared healthy even after 600 days after infection, indicating that Δ*kasB* had failed to cause active infection in the mice. Surprisingly, unlike the results obtained with C57BL/6 mice, the Δ*kasB* strain caused mortality in immunodeficient SCID mice (SI Fig. 15).

Discussion

Our studies demonstrate that the FASII β-ketoacyl-ACP synthase KasB is essential for full MA chain length in *M. tuberculosis*. Although the results of *in vitro* assays suggested that KasB may be involved in elongating a major portion of the mero-MA chain (14), deletion of *kasB* resulted in the shortening of the mero-MA chains by only 2–6 carbons. In addition, the Δ*kasB* mutant lost the ability to synthesize any *trans*-cyclopropanated keto-MAs and produced a miniscule amount of *trans*-cyclopropanated methoxy-MAs, accumulating instead their corresponding unsaturated precursors with *trans*-double bonds, which are putative substrates of the *trans*-cyclopropane synthase CmaA2 (18). This unexpected consequence of *kasB* deletion meant that either the shortened oxygenated mero-MAs are poor substrates for CmaA2 or that CmaA2 interacts preferentially with KasB present in specialized FASIIs, as recently suggested (28, 29). Thus, the deletion of *kasB* had a "downstream phenotypic" effect on *trans*-cyclopropanation of oxygenated MAs, an activity not directly associated with KasB function. In addition, the proportions of the different MA species were also altered, with a reduction in the levels of keto-MAs. These alterations in structure (shortening of MA chain length and loss or reduction of *trans*-cyclopropanation) and in content (reduction in keto-MAs) were observed for both wall-bound and trehalose-bound MAs (data not shown).

Our findings have similarities but also several differences compared with those reported for a transposon-disrupted *kasB* mutant of *M. marinum* (13). In that study, MA species 4 carbons shorter were found compared with up to 6 carbons shorter in the *M. tuberculosis* mutant. We also observed that the deletion of *kasB* affected MA *trans*-cyclopropanation, an activity not detected in WT *M. marinum*. And finally, unlike the *M. marinum* mutant study, we were able to test the ability of the *M. tuberculosis* Δ*kasB* mutant to cause infection in an animal model of infection and thus assess the role of KasB in virulence.

A remarkable change in Δ*kasB* was the complete loss of the acid-fast staining property that is one of the primary defining characteristics of *M. tuberculosis*. Loss of acid-fastness by Δ*kasB* was not only observed in broth cultures but also in infected murine lung tissue. Here again, direct or indirect effects of changes in the MAs of the *kasB* mutant, like a decrease in lipophilicity, may have rendered the cell wall more prone to decolorization with acid-alcohol. It is unlikely that any specific chemical interactions of MAs with the primary stain that were lost in Δ*kasB* could have been responsible for the loss of acid-fastness because two different staining methods (using chemically distinct primary stains) yielded the same results. This work reports the loss of acid-fastness in a specific *M. tuberculosis* mutant that is defective in normal MA biosynthesis, and the only other well characterized acid-fast negative *M. tuberculosis* mutant described has a deletion in *phoP*, which leads to deficiencies of many lipids, including sulfatides, diacyltrehaloses, and polyacyltrehaloses (30). It is worth noting that the deletion of *cmaA2* in *M. tuberculosis* did not alter colony morphology, cording, or acid-fastness (18), indicating that loss of or reduction in *trans*-cyclopropanation can be ruled out as a potential cause of the observed phenotypes in Δ*kasB*.

TDMs are believed to play a particularly important role in determining colony characteristics and cording (31), and the observed changes in colony morphology and cording in the Δ*kasB* mutant were thus likely a direct or indirect effect of the altered MA profile of the TDMs produced by the mutant. Loss of cording is often associated with decreased virulence (19), and indeed this was the case with the Δ*kasB* mutant. Before these studies, three other *M. tuberculosis* mutants defective in MA biosynthesis had been tested in the mouse model of infection: Δ*mma4* and Δ*pcaA* were found to be attenuated (16, 19), whereas Δ*cmaA2* was hypervirulent (32). Although Δ*pcaA* and Δ*mmaA4* showed reduced replication in mouse organs, moderately high numbers of bacteria could be found in the lungs, spleen, and liver of mice even 20–30 weeks after infection (albeit lower than those found for the WT strain) (16, 19). None of these three mutants has been reported as acid-fast negative, and only the Δ*pcaA* mutant was defective in cording.

The Δ*kasB* mutant displayed a number of interesting *in vivo* phenotypes. First, it was severely attenuated for growth in immunocompetent C57BL/6 mice: the mutant did initially colonize lung, liver, and spleen in infected immunocompetent C57BL/6 mice; determination of bacterial loads in organs and histological examination of tissue sections revealed that Δ*kasB* failed to replicate to the levels normally observed in these tissues and did not cause the pathology usually associated with *M. tuberculosis* infection.

Perhaps the most striking *in vivo* phenotype of the Δ*kasB* mutant was its ability to persist at constant low levels in lungs and spleen for 450 days after aerosol infection. The mutant also failed to cause active disease in the mice: Δ*kasB*-infected mice appeared healthy even 600 days after infection. In contrast, SCID mice succumbed to infection by Δ*kasB*, indicating a clear role for cell-mediated immunity in the control of replication of the Δ*kasB* mutant. The absence of any differences between WT and Δ*kasB* in regard to their ability to survive in macrophages suggests that early defense mechanisms, like intracellular oxidative damage in macrophages, did not play a role in the attenuation of the mutant strain. Thus, the surprising "hypovirulence" of Δ*kasB* could be a consequence of a number of other factors resulting from the altered MA profile and their effects on the interaction of the bacteria with the host adaptive immune system. One possibility is the exposure of cell envelope components, normally "masked" in WT strains, which may induce a more robust immune response. Another possibility is the modulation of the immune response by cell wall components; TDMs are the major cell wall glycolipids and are known to modulate the immune response (32, 33). It is therefore likely that Δ*kasB* TDMs containing altered MAs modulate innate and adaptive immune responses, resulting in the observed *in vivo* growth defect.

A third of the human population is latently infected with the tubercle bacillus, and this dormant, drug-tolerant stage of the bacterium is a major challenge for the tuberculosis therapy and control. Although this latency provides an important reservoir for disease reactivation, very little is known about bacterial and host factors that are involved in long-term persistence. The long-term persistence of Δ*kasB* for up to 600 days in immunocompetent mice without causing disease suggests that the mutant strain can provide a good model for studying latent *M. tuberculosis* infection. Furthermore, this unique *in vivo* phenotype makes *kasB* an attractive candidate for deletion in a live attenuated vaccine strain.

The increased sensitivity of the *kasB* mutant to lipophilic antibiotics highlights the attractiveness of KasB as an important secondary drug target in combination therapy. Specific inhibitors of KasB could be envisioned as inhibiting long-chain mero-MA biosynthesis and, as a result, attenuating *M. tuberculosis* while at the same time making the bacterium even more susceptible to drugs such as rifampicin used in combination. In addition to an increased permeability to lipophilic drugs, the increased sensitivity of Δ*kasB* to thiolactomycin, a drug known to inhibit both KasA and KasB (34), may have been due to a lesser titration of the drug as a result of the absence of KasB.

In summary, our studies have demonstrated that KasB-mediated elongation of MAs is crucial for cording, acid-fast staining, subsequent *trans*-cyclopropanation, and the ability of *M. tuberculosis* to cause disease in immunocompetent mice. Our findings have important implications for understanding and solving the problems of latency and antibiotic tolerance in *M. tuberculosis* infection.

Materials and Methods

Plasmids and Phages. Plasmids and phages used in this work are outlined in SI Table 2. Slow-growing mycobacteria were cultured in 7H9 broth (Difco, Sparks, MD) containing 10% Middlebrook OADC enrichment and 0.05% Tween 80, on 7H9 agar (made by adding 1.5% agar to OADC-enriched 7H9 broth), or on Middlebrook 7H10 agar (Difco). *Escherichia coli* strains were cultured in LB broth. The concentrations of antibiotics used were 75 μg/ml hygromycin and 20 μg/ml kanamycin for mycobacterial strains, and 150 μg/ml hygromycin and 40 μg/ml kanamycin for *E. coli*.

Construction of Deletion Mutants. For generating an allelic exchange construct designed to replace the *kasB* gene with a hygromycin resistance cassette (*hyg*), 500-bp sequences flanking the left and right of the *M. tuberculosis kasB* gene were PCR-amplified from pYUB2271 (a cosmid vector containing *kasB*) using the primer pairs MtKasB1 (5′-GCGACTAGTGGTAGGGCGATGACTCGC-3′) and MtKasB2 (5′-CGTATGCATACCAGCTCCGTCATTG-3′), and MtKasB3 (5′-GCGTCTAGAGAGATCGATTTGGACGTG-3′) and MtKasB4 (5′-GCAGGTACCACCGAGATCTGCGGGATG-3′), respectively. After cloning into pCR2.1-TOPO and sequencing, the cloned PCR fragments were excised by using the primer-introduced restriction sites and cloned into the allelic exchange plasmid vector pJSC347 (SI Table 2). The resultant plasmid, pYUB2417, was then packaged into the temperature-sensitive phage phAE159 (J. Kriakov and W.R.J., Jr., unpublished results), as described (35), to yield the *kasB*-knockout phage phAE404. Specialized transduction was performed as described (35).

Biochemical Analyses of MAs and Lipids. TLC analysis of MAs was done as described (23, 34). MA extraction and derivatization for TLC analysis, and purification for MS and NMR analysis, were

done as described (19, 36). In brief, MAs of each strain were liberated by alkali hydrolysis (10% KOH/methanol, wt/vol) from the heat-killed bacteria at 90°C for 2 h, followed by extraction with *n*-hexane. After methylation with diazomethane, each subclass, α-, methoxy-, and keto-MAME, was purified by preparative TLC of silica gel until a single spot was obtained. The developing system was benzene or *n*-hexane/diethyl ether (90:15, vol/vol). The molecular species of the MAMEs were detected by MALDI-TOF MS by using an Ultraflex II (Bruker Daltonics, Billerica, MA). The purified MAMEs were prepared in chloroform at a concentration of 1 mg/ml, and a droplet of a 1-μl sample was applied directly on the sample plate followed by 1 μl of matrix solution (2,5-dihydroxybenzoic acid/10 mg/ml in chloroform/methanol, 1:1 vol/vol). MAMEs were analyzed in the Reflectron mode with an accelerating voltage operating in positive mode of 20 kV. An external mass calibration was performed by peptide calibration standard II (Bruker Daltonics), including known peptide standards in a mass range from 700 to 4,000 Da (15). ^{1}H NMR spectra of MAMEs were obtained in $CDCl_3$ (100% D) by using a Bruker Avance 600 spectrometer at 25°C. Chemical shift values (in ppm) were relative to internal $CHCl_3$ resonance (at 7.26 ppm). Pyrolysis and subsequent GC-MS of MAs was done in accordance with published methods (37, 38). Lipid extraction and TLC analysis were done as described (39).

Mouse Infections. C57BL/6 mice were exposed to aerosols of different strains of *M. tuberculosis* in an aerosolization chamber. A suspension of 10^6 cfu/ml in PBS containing 0.05% Tween 80 and 0.004% antifoam was used as the inoculum to obtain ≈100 cfu per lung. Four mice from each infection group were killed 24 h after infection, and lung homogenates were plated on 7H9-agar plates to determine the efficiency of aerosolization. At different time points, three or four mice were killed from each infection group to determine bacterial loads in the spleen, lung, and liver. Eight mice from each group were also used to determine survival times of infected mice. Pathological analysis and histological staining of organ sections were done on tissues fixed in buffered 10% formalin.

We thank Annie Dai, Mei Chen, and John Kim for technical assistance; Jordan Kriakov (Albert Einstein College of Medicine) for providing phAE159; Howard Steinman for helpful comments; and Matsumi Doe, Shinji Maeda, and Takashi Naka of Osaka City University for technical support. This work was supported by Howard Hughes Medical Institute and National Institutes of Health Grants AI063537 (to W.R.J.) and AI26170 (to W.R.J., S.A.P and J.C.); Center for AIDS Research Grant AI051519; Grants H12-Shinko-30, H16-Shinko-1 and H18-Shinko-11 from the Ministry of Health, Labor, and Welfare in Japan (to N.F. and K.K.); a grant from the Medical Research Council and the Wellcome Trust, U.K. (to G.S.B.); and Centre National de la Recherche Scientifique CNRS ATIP "Microbiologie Fondamentale" (to L.K.). G.S.B. acknowledges support from Mr. James Bardrick in the form of a Personal Research Chair, and as a former Lister Institute-Jenner Research Fellow. A.B. acknowledges support from the Medical Research Council (U.K.) in the form of Career Development Award G0600105 at the University of Birmingham.

1. Trebucq A (2004) *Int J Tuberc Lung Dis* 8:805.
2. Bishop PJ, Neumann G (1970) *Tubercle* 51:196–206.
3. Neelsen F (1883) *Centralbl Med Wissen* 28:497.
4. Ziehl F (1882) *Deut Med Wochen* 8:451.
5. Goren MB, Cernich M, Brokl O (1978) *Am Rev Respir Dis* 118:151–154.
6. Harada K (1976) *Stain Technol* 51:255–260.
7. Murohashi T, Kondo E, Yoshida K (1969) *Am Rev Respir Dis* 99:794–798.
8. Koch-Weser D, Barclay WR, Ebert RH (1955) *Am Rev Tuberc* 71:556–565.
9. Besra GS, Sievert T, Lee RE, Slayden RA, Brennan PJ, Takayama K (1994) *Proc Natl Acad Sci USA* 91:12735–12739.
10. Brennan PJ, Nikaido H (1995) *Annu Rev Biochem* 64:29–63.
11. Cole ST, Brosch R, Parkhill J, Garnier T, Churcher C, Harris D, Gordon SV, Eiglmeier K, Gas S, Barry CE, III, *et al*. (1998) *Nature* 393:537–544.
12. Bhatt A, Kremer L, Dai AZ, Sacchettini JC, Jacobs WR, Jr (2005) *J Bacteriol* 187:7596–7606.
13. Gao LY, Laval F, Lawson EH, Groger RK, Woodruff A, Morisaki JH, Cox JS, Daffe M, Brown EJ (2003) *Mol Microbiol* 49:1547–1563.
14. Slayden RA, Barry CE, III (2002) *Tuberculosis* 82:149–160.
15. Dinadayala P, Laval F, Raynaud C, Lemassu A, Laneelle MA, Laneelle G, Daffe M (2003) *J Biol Chem* 278:7310–7319.
16. Dubnau E, Chan J, Raynaud C, Mohan VP, Laneelle MA, Yu K, Quemard A, Smith I, Daffe M (2000) *Mol Microbiol* 36:630–637.
17. Glickman MS (2003) *J Biol Chem* 278:7844–7849.
18. Glickman MS, Cahill SM, Jacobs WR, Jr (2001) *J Biol Chem* 276:2228–2233.
19. Glickman MS, Cox JS, Jacobs WR, Jr (2000) *Mol Cell* 5:717–727.
20. Takayama K, Wang C, Besra GS (2005) *Clin Microbiol Rev* 18:81–101.
21. Yuan Y, Barry CE, III (1996) *Proc Natl Acad Sci USA* 93:12828–12833.
22. Yuan Y, Crane DC, Musser JM, Sreevatsan S, Barry CE, III (1997) *J Biol Chem* 272:10041–10049.
23. Kremer L, Guerardel Y, Gurcha SS, Locht C, Besra GS (2002) *Microbiology* 148:3145–3154.
24. George KM, Yuan Y, Sherman DR, Barry CE, III (1995) *J Biol Chem* 270:27292–27298.
25. Watanabe M, Aoyagi Y, Ridell M, Minnikin DE (2001) *Microbiology* 147:1825–1837.
26. Astola J, Munoz M, Sempere M, Coll P, Luquin M, Valero-Guillen PL (2002) *Microbiology* 148:3119–3127.
27. Watanabe M, Ohta A, Sasaki S, Minnikin DE (1999) *J Bacteriol* 181:2293–2297.
28. Veyron-Churlet R, Bigot S, Guerrini O, Verdoux S, Malaga W, Daffe M, Zerbib D (2005) *J Mol Biol* 353:847–858.
29. Veyron-Churlet R, Guerrini O, Mourey L, Daffe M, Zerbib D (2004) *Mol Microbiol* 54:1161–1172.
30. Walters SB, Dubnau E, Kolesnikova I, Laval F, Daffe M, Smith I (2006) *Mol Microbiol* 60:312–330.
31. Hunter RL, Venkataprasad N, Olsen MR (2006) *Tuberculosis* 86:349–356.
32. Rao V, Gao F, Chen B, Jacobs WR, Jr, Glickman MS (2006) *J Clin Invest* 116:1660–1667.
33. Rao V, Fujiwara N, Porcelli SA, Glickman MS (2005) *J Exp Med* 201:535–543.
34. Kremer L, Douglas JD, Baulard AR, Morehouse C, Guy MR, Alland D, Dover LG, Lakey JH, Jacobs WR, Jr, Brennan PJ, *et al*. (2000) *J Biol Chem* 275:16857–16864.
35. Bardarov S, Bardarov S, Jr, Pavelka MS, Jr, Sambandamurthy V, Larsen M, Tufariello J, Chan J, Hatfull G, Jacobs WR, Jr (2002) *Microbiology* 148:3007–3017.
36. Fujiwara N, Pan J, Enomoto K, Terano Y, Honda T, Yano I (1999) *FEMS Immunol Med Microbiol* 24:141–149.
37. Guerrant GO, Lambert MA, Moss CW (1981) *J Clin Microbiol* 13:899–907.
38. Kaneda K, Imaizumi S, Yano I (1995) *Microbiol Immunol* 39:563–570.
39. Dobson G, Minnikin DE, Minnikin SM, Parlett M, Goodfellow M, Ridell M, Magnusson M (1985) in *Chemical Methods in Bacterial Systematics*, eds Goodfellow M, Minnikin DE (Academic, London), pp 237–265.